

Circulating exosomal microRNA-4497 as a potential biomarker for metastasis and prognosis in non-small-cell lung cancer

Bokun Zheng^{1,2*} , Mingcheng Peng^{1,2*}, Jun Gong³, Changsheng Li⁴, Hongbing Cheng⁵, Yirong Li^{1,2} and Yueting Tang^{1,2}

¹Department of Clinical Laboratory, Zhongnan Hospital of Wuhan University, Wuhan, Hubei 430071, China; ²Wuhan Research Center for Infectious Diseases and Cancer, Chinese Academy of Medical Sciences, Wuhan, Hubei 430071, China; ³Department of Radiation and Medical Oncology, Zhongnan Hospital of Wuhan University, Wuhan, Hubei 430071, China; ⁴Department of Thoracic Surgery, Zhongnan Hospital of Wuhan University, Wuhan, Hubei 430071, China; ⁵Department of Thoracic Surgery, Xiantao First People's Hospital Affiliated to Yangtze University, Xiantao, Hubei 433099, China

*These authors contributed equally to this paper.

Corresponding authors: Yirong Li. Email: liyirong838@163.com; Yueting Tang. Email: anzhitinglan723@sina.com

Impact Statement

Most studies on miR-4497 in tumors have focused on its mechanism of action, and few have reported that exosomal miR-4497 could be a circulating biomarker. Moreover, most traditional biomarkers are tumor promoters and do not have sufficient diagnostic value for lung cancer. We are the first research group to study the expression characteristics of miR-4497 in circulating exosomes in non-small-cell lung cancer (NSCLC), which showed excellent tumor suppressor effects in the identification of multiple models, whether in early screening to identify NSCLC patients, BLL patients, and healthy people or for staging and grading, prognosis, and monitoring recurrence, metastasis, and the therapeutic effects in NSCLC patients. Moreover, serum exosomal miR-4497 is an independent tumor suppressor, and its combination with tumor markers can yield high diagnostic accuracy in different models. Therefore, our study suggests that serum exosomal miR-4497 has excellent clinical application value and provides valuable information for physicians to diagnose and treat patients with NSCLC.

Abstract

Circulating exosomal microRNAs (miRNAs) have shown great potential for the diagnosis, prognosis, and treatment monitoring of patients with non-small-cell lung cancer (NSCLC). Our main purpose was to determine the clinical value of serum exosomal miR-4497 as a new non-invasive biomarker for NSCLC. The exoRNeasy Kit (QIAGEN, Hilden, Germany) was used to isolate exosomes and exoRNA from the serum of 84 patients with NSCLC (NSCLC group), 30 patients with benign lung lesion (BLL group), and 47 healthy controls. Six serum exosomal miRNAs (Let-7b-5p, miR-122-5p, miR-155-5p, miR-223-3p, miR-320c, and miR-4497) were selected as candidate miRNAs and analyzed using real-time qPCR, among which miR-4497 displayed the most striking differences. Exosomal miR-4497 expressed significantly lower in NSCLC than in BLL patients and healthy controls ($P < 0.001$). Further investigation showed that miR-4497 was negatively correlated with the malignant characteristics of tumors (tumor size, tumor–node–metastasis [TNM] stage, and distant metastasis) and was an independent tumor suppressor ($P < 0.05$). According to receiver operating characteristic (ROC) analysis, exosomal miR-4497 independently exhibited excellent diagnostic efficacy, which could be improved by combining it with traditional markers (for identifying tumor size, the area under the curve [AUC]=0.761; TNM stage, AUC=0.878; distant metastasis, AUC=0.895; all $P < 0.001$). Moreover, longitudinal analysis revealed that exosomal miR-4497 levels increased after chemoradiotherapy ($P < 0.001$). According to the survival analysis, poor overall survival (OS) and disease-free survival (DFS) were associated with low exosomal miR-4497 levels ($P < 0.05$). Moreover, exosomal miR-4497 was an independent protective factor affecting DFS (hazard ratio=0.190, $P=0.009$) in the

Cox proportional hazards model. Therefore, serum exosomal miR-4497 can be used as a potential biomarker to identify NSCLC and healthy individuals or BLL patients for early screening or as a biomarker for staging and grading, prognosis, and monitoring recurrence, metastasis, and the therapeutic effects in patients with NSCLC.

Keywords: miR-4497, exosome, non-small-cell lung cancer, circulating biomarker, metastasis, prognosis

Experimental Biology and Medicine 2023; 248: 1403–1413. DOI: 10.1177/15353702231184223

Introduction

Lung cancer (LC) is the most common type of malignancy and the main cause of cancer-related deaths worldwide.¹

Non-small-cell lung cancer (NSCLC) accounts for approximately 85% of all types of LC.² As with other cancers, LC tends to be asymptomatic for prolonged periods, infiltrates surrounding tissues, and metastasizes to distant organs.³

Unfortunately, many patients are diagnosed at later stages, resulting in unfavorable outcomes and poor survival.² These phenomena highlight the urgent need to identify and develop powerful, sensitive, and non-invasive screening biomarkers that facilitate early diagnosis and dynamic monitoring of recurrence and distant metastasis of NSCLC.⁴ For example, the liquid biopsies based on blood and body fluid contents, cell-free DNA,⁵ circulating tumor cells,⁶ and exosomes were included in a previous study.⁷

Exosomes are membrane vesicles with a diameter of 30–150 nm secreted by different cells under physiological and pathological conditions⁸ and act as essential messengers in cancer by delivering the cargo of vesicles (such as lipids, proteins, or nucleic acids) to specific recipient cells.⁹ Numerous reports have indicated that in the tumor microenvironment, exosomes secreted by tumor cells interact with different cell types to regulate tumor occurrence and development, angiogenesis, metastasis, and immune escape.¹⁰ Furthermore, exosomes are abundantly and naturally found in bodily fluids, reaching all parts of the human body through peripheral circulation and mediating cell-to-cell communication.¹¹ Thus, circulating exosomes can be used as liquid biopsies and non-invasive biomarkers for early detection, diagnosis, and treatment.¹²

MicroRNAs (miRNAs) include approximately 18–25 nt endogenous RNAs and play vital roles in gene regulation. They guide the post-transcriptional repression of protein-coding genes by pairing them with their mRNAs.¹³ Cell-derived exosomes are taken up by adjacent or distant cells, and the contained miRNAs are released. These miRNAs regulate the tumor microenvironment and immune processes that contribute to tumor occurrence, invasion, migration, angiogenesis, and drug resistance.¹⁴ Notably, in exosomes, specific oncogenic and tumor suppressor miRNAs have potential for diagnosis or prognosis and can be used as non-invasive markers for a variety of cancers, including NSCLC.¹⁴

In our previous study, we identified the unique miRNA profiles of LC cell-derived exosomes.¹⁵ To explore whether the exosomal miRNAs discovered *in vitro* can be used to diagnose and monitor metastasis for LC *in vivo*, 13 exosomal miRNAs, including miR-27b-3p, miR-423-3p, miR-122-5p, miR-132-3p, miR-192-5p, miR-155-5p, miR-223-3p, miR-320c, miR-576-3p, miR-1290, miR-1246, miR-4497, and Let-7b-5p, were selected and screened based on our *in vitro* studies,¹⁵ other literature reports,^{16–19} and detectability in human serum samples. From these investigations, six (Let-7b-5p, miR-122-5p, miR-155-5p, miR-223-3p, miR-320c, and miR-4497) showed dysregulated expression levels in serum exosomes of NSCLC patients. Interestingly, miR-4497 displayed the most striking differences among the miRNAs examined in this study, which warrants further investigation. Other studies have reported that the upregulation of miR-4497 enhances the killing effect of radiation therapy in NSCLC by silencing MED131 and inhibiting PRKCA expression.²⁰ Notably, no studies have explored the application value of serum exosomal miR-4497 in clinical settings for NSCLC patients. Therefore, our research aimed to analyze the expression characteristics of exosomal miR-4497 with varying severity and disease course and evaluate its value as

a novel biomarker for NSCLC diagnosis, metastasis monitoring, and prognosis evaluation.

Materials and methods

Study population and preparation of serum samples

In total, 84 patients with NSCLC, 30 patients with a benign lung lesion (BLL), and 47 age- and sex-matched healthy controls (HCs) were enrolled from Zhongnan Hospital of Wuhan University and Xiantao First People's Hospital of Yangtze University between July 2017 and December 2022. The use of patient samples was approved by the Ethics Committee of Zhongnan Hospital of Wuhan University (2017059), and written informed consent was obtained from each participant. We divided the NSCLC patients into paired pretreatment and post-treatment groups. Paired serum samples were collected during the two treatment stages. None of the NSCLC patients in the pretreatment group had received any surgery, radiotherapy, or chemotherapy. All NSCLC cases were pathologically confirmed by two independent pathologists. NSCLC staging was determined using the American Joint Committee on Cancer staging handbook. Information on all NSCLC patients was retrospectively collected from a clinical database and is summarized in Table 1. The BLL group included patients who were pathologically diagnosed with granulomas or inflammatory changes. HCs were selected from populations who underwent regular physical examination. Patients with a history of smoking, genotoxic therapies, tumors, increased serum tumor marker levels, or abnormal radiologic imaging results were excluded.

The samples were collected and processed according to the approved guidelines. Blood samples collected from participants and were centrifuged at 3000 g for 15 min, and the serum supernatant was frozen at -80°C until the next procedure.

Exosome and exoRNA extraction

Serum exosomes were extracted using the exoRNeasy Serum/Plasma Midi Kit (QIAGEN, Hilden, Germany). Serum samples were thawed on ice, and then centrifuged at 16,000g and 4°C for 10 min, with the aim of removing cell debris and coagulated protein. Next, 500 μL of each sample was used for exosome and exoRNA extraction. Using a procedure modified based on the exoRNeasy protocol, the total RNA of exosome (exoRNA) from the 500 μL of prefiltered serum was isolated. To characterize the exosomes, 500 μL buffer XE was added to the spin column membrane and incubated at 25°C for 5 min, followed by centrifugation at 500g for 5 min; the exosomes were eluted and suspended in $1\times$ phosphate-buffered saline (PBS).

Nanoparticle tracking analysis

The size distribution and concentration of exosomes were determined by nanoparticle tracking analysis (NTA) using a ZetaView particle tracker (Particle Metrix, Inning am Ammersee, Germany) equipped with a 488-nm laser. Each sample was measured three times, 30 frames were captured

Table 1. Correlation between serum exosomal miR-4497 levels and clinical characteristics in NSCLC.

	Number	miR-4497	<i>P</i> value
Age (years)			0.812
<60	28	0.439 ± 0.080	
≥60	56	0.483 ± 0.066	
Gender			0.489
Male	61	0.469 ± 0.065	
Female	23	0.466 ± 0.074	
Smoking history			0.833
Yes	27	0.453 ± 0.085	
No	57	0.475 ± 0.065	
Hypertension			0.811
Yes	17	0.401 ± 0.081	
No	67	0.485 ± 0.061	
Diabetes mellitus			0.406
Yes	12	0.531 ± 0.121	
No	72	0.458 ± 0.057	
Primary location			0.800
Left lung	32	0.447 ± 0.799	
Right lung	52	0.481 ± 0.068	
Tumor size			0.001
≤3 cm	28	0.652 ± 0.090	
>3 cm	56	0.376 ± 0.060	
Pathological classification			0.680
LUAD	28	0.452 ± 0.053	
SCC	56	0.501 ± 0.112	
Mutation			0.069
Yes	19	0.289 ± 0.056	
No	65	0.521 ± 0.063	
TNM stage			0.001
I-II	42	0.623 ± 0.084	
III-IV	42	0.313 ± 0.050	
Lymph node metastasis			0.125
Yes	44	0.401 ± 0.069	
No	40	0.542 ± 0.076	
Distant metastasis			<0.001
Yes	24	0.204 ± 0.041	
No	60	0.574 ± 0.065	

NSCLC: non-small-cell lung cancer; TNM: tumor–node–metastasis; LUAD: lung adenocarcinoma; SCC: squamous cell carcinoma. All data with *P* value of <0.05 are bolded and italicized. Data are mean ± SEM. *P* values are from Mann–Whitney *U* test. *P* < 0.05 was considered statistically significant. Data were available for 44 patients.

at each position, and the results were statistically analyzed using ZetaView Software (version 8.05.11 SP1).

Transmission electron microscopy

A 1% phosphotungstic acid solution (pH 6.8) was used to post-negatively stain the exosome solution, which was then added to copper grids for 2 min. The liquid was absorbed using a filter paper along the edges of the copper grids and an incandescent lamp was used to dry the grid for 10 min. The grids were observed and images captured using a Tecnai 12 transmission electron microscope (FEI; Eindhoven, the Netherlands).

Western blotting

Concentrated exosome supernatants or A549 cells (positive control) were lysed using RIPA lysis solution (Biosharp,

Beijing, China). Western blotting was performed 10% sodium dodecyl sulfate-polyacrylamide gel electrophoresis (SDS-PAGE) electrophoresis to separate 50 µg protein from each sample. Polyvinylidene fluoride (PVDF) membranes (Biosharp, Beijing, China) were incubated with rabbit primary antibodies against CD63 (Abcam, Cambridge, UK), CD9 (Abcam), TSG101 (Abcam), and calnexin (Bioworld Technology, St. Louis Park, MN, USA) and horseradish peroxidase (HRP)-conjugated anti-rabbit antibodies (Proteintech, Wuhan, China). Finally, immunoreactive bands were detected using an ECL blotting detection reagent (Bio-Rad, Hercules, CA, USA).

Relative quantification of miRNA

During exoRNA isolation, as described in the previous section (i.e. Exosome and exoRNA extraction), 25 fmol synthetic *Caenorhabditis elegans* miRNA cel-miR-39 was used as a spike-in control miRNA. Purified RNA (<1000 ng) was reverse-transcribed according to the manufacturer's instructions into complementary DNA (cDNA) using the All-in-One™ miRNA First-Strand cDNA Synthesis Kit (GeneCopoeia, Rockville, MD, USA) on a Bio-Rad T100 thermal cycler. The reaction mixture was incubated at 37°C for 60 min, followed by 85°C for 5 s and 4°C for 60 min. Using the All-in-One miRNA qPCR Kit (GeneCopoeia) to perform qRT-PCR in a 25-µL reaction system. Reactions were performed using a Bio-Rad CFX96 qPCR System. In short, 10 min after the initial denaturation step at 95°C, 40 cycles of amplifications were performed for 10 s at the melting temperature of 95°C and 20 s at the annealing temperature of 60°C. The specificity of the PCR products was evaluated using melting curves. The miRNA-specific primer sequences were purchased from GeneCopoeia. We used the 2^{-ΔΔCt} relative quantification method to compare the miRNA expression levels.

Statistical analysis

SPSS 26.0 (IBM Corp., Armonk, NY, USA) was used for statistical analysis. Serum exosomal miRNA levels were assessed in different groups using Mann–Whitney *U* or Kruskal–Wallis tests, and differences between paired values were assessed using the Wilcoxon signed-rank test. Binary logistic regression analysis identified independent factors affecting NSCLC parameters (tumor size, tumor–node–metastasis [TNM] stage, lymph node metastasis [LNM], and distant metastasis). Diagnostic efficacy was evaluated based on the area under the curve (AUC) and receiver operating characteristic (ROC) curves. The Kaplan–Meier method and log-rank test were used to determine the survival curves. Finally, univariate and multivariate Cox proportional hazards model analyses were used to identify the prognostic factors. Statistical significance was set at *P* < 0.05.

Results

Characterization of serum-derived exosomes

The exosome nanoparticles mainly ranged between 50 and 200 nm in diameter with a concentration of approximately 3.7 × 10¹¹, as shown by the ZetaView analysis (Figure 1(A)).

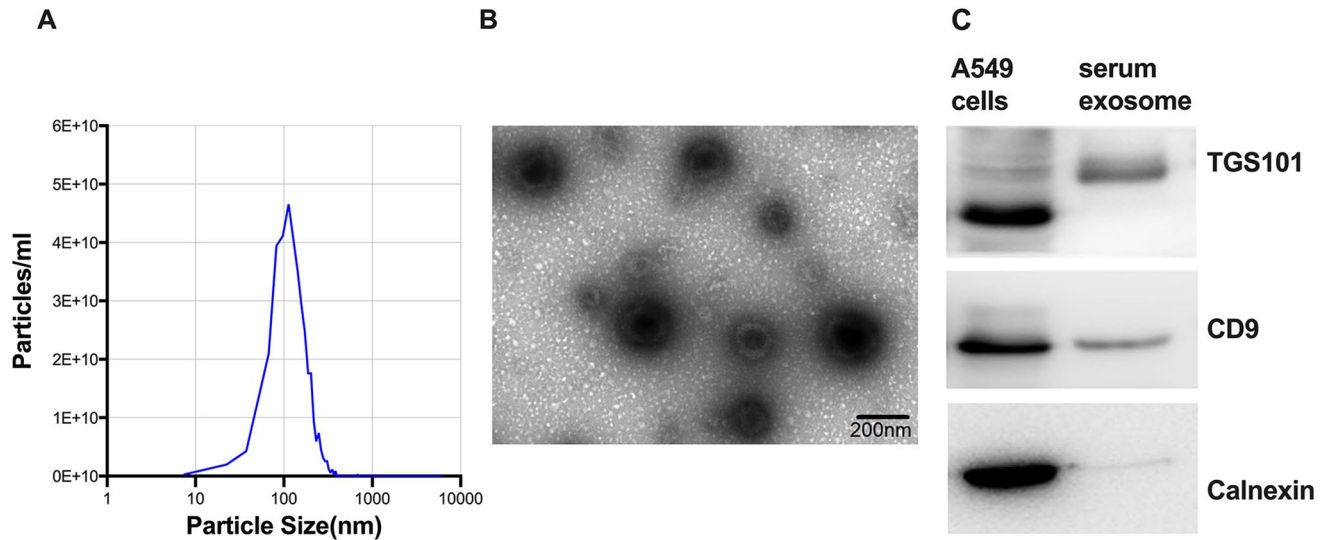


Figure 1. Characterization of exosomes. (A) NTA analysis by ZetaView particle tracker showed that the size distribution of exosomes was 50–200 nm. (B) Exosomes were visualized by TEM. (C) The detection of TSG101, CD9, and calnexin as exosomal markers using Western blotting.

In addition, transmission electron microscopy (TEM) showed that the exosomes were spherical in shape (Figure 1(B)). Furthermore, CD9 and TSG101, two well-known protein markers, were detected in the exosomes. However, only the negative control, calnexin, was found in the cells (Figure 1(C)). These results indicate that exosomes were successfully obtained using the exoRNeasy Serum/Plasma Midi Kit.

Expression of several serum exosomal miRNAs in NSCLC

Based on qRT-PCR results, six exosomal miRNAs (Figure 2) were selected as candidate miRNAs. The data indicated that the expression of serum exosomal let-7b-5p in the NSCLC groups was significantly higher than that in the HC group (NSCLC vs HC: 2.001 ± 0.205 vs 1.391 ± 0.240 , $P < 0.01$) (Figure 2(A)). Compared with the HC group, the following were significantly decreased in the NSCLC groups: serum exosomal miR-122-5p (NSCLC vs HC: 1.075 ± 0.216 vs 2.440 ± 0.558 , $P = 0.027$) (Figure 2(B)); miR-155-5p (0.358 ± 0.072 vs 3.767 ± 1.239 , $P < 0.001$) (Figure 2(C)); miR-223-3p (0.629 ± 0.082 vs 5.673 ± 3.860 , $P = 0.013$) (Figure 2(D)); miR-320c (0.753 ± 0.117 vs 2.695 ± 0.706 , $P = 0.025$) (Figure 2(E)); and miR-4497 (0.370 ± 0.056 vs 1.260 ± 0.167 , $P < 0.001$) (Figure 2(F)). Among these, the significant difference in miR-4497 expression was the largest and most stable; therefore, we performed further analyses.

Exosomal miR-4497 is downregulated in NSCLC and as a tumor suppressor in tumor size, TNM stage, and metastasis

We further expanded the sample size of NSCLC patients and HCs and then added the BLL patients. The results exhibited that the expression of exosomal miR-4497 in NSCLC was significantly lower compared with the BLL and HC groups (HC vs stage I–II vs stage III–IV: 1.178 ± 0.105 vs 0.623 ± 0.084 vs 0.313 ± 0.050 , $P < 0.01$) (BLL vs stage I–II vs stage III–IV: 0.943 ± 0.103 vs 0.623 ± 0.084 vs 0.313 ± 0.050 , $P < 0.05$) (Figure 3(A)).

Moreover, we studied the relationship between serum exosomal miR-4497 and the clinicopathological characteristics of NSCLC (Table 1). No significant associations were identified between miR-4497 and age, sex, smoking status, comorbidities, primary tumor location, pathological classification, mutation, or LNM ($P > 0.05$). Notably, our main finding was that exosomal miR-4497 expression was correlated with TNM stage (Figure 3(A)), tumor size (Figure 3(B)), and distant metastasis (Figure 3(C)). Specifically, NSCLC patients with advanced clinical stages (III–IV) had lower levels of serum exosomal miR-4497 compared with controls (I–II) ($P = 0.001$). Patients with low serum exosomal miRNA-4497 had larger tumor sizes (≤ 3 cm vs > 3 cm: 0.652 ± 0.090 vs 0.376 ± 0.060 , $P = 0.001$). Similarly, our results revealed that the exosomal miR-4497 showed lower expression levels in the patients with distant metastasis (M0 vs M1: 0.574 ± 0.065 vs 0.204 ± 0.041 , $P < 0.001$).

Binary logistic regression analysis was performed to determine whether miR-4497 and other risk factors independently affect NSCLC progression (Table 2). We defined the binary dependent variables according to tumor size (Model 1), TNM stage (Model 2), LNM (Model 3), or distant metastasis (Model 4), and seven factors, including age, sex, smoking history, miR-4497, and other traditional tumor markers (carcinoembryonic antigen [CEA], neuron-specific enolase [NSE], and CA-125), were qualified as covariates for the multivariate analysis. In Model 1, the combination of smoking history (odds ratio [OR], 4.688; 95% confidence interval [CI]: 1.337–16.438, $P = 0.016$) and miR-4497 expression (OR, 0.243; 95% CI: 0.074–0.793, $P = 0.019$) was screened as the optimal panel. In Model 2, NSE (OR: 1.263, 95% CI: 1.0085–1.469, $P = 0.003$), CA125 (OR: 1.077, 95% CI: 1.023–1.134, $P = 0.005$), and miR-4497 (OR: 0.155, 95% CI: 0.034–0.709, $P = 0.016$) entered the logistic regression equation. In Model 3, the panel of NSE (OR: 1.144, 95% CI: 1.021–1.269, $P = 0.011$) and CA125 (OR: 1.055, 95% CI: 1.015–1.097, $P = 0.007$) was selected as the best combination. In Model 4, NSE (OR: 1.163, 95% CI: 1.036–1.306, $P = 0.010$), CA125 (OR: 1.013, 95% CI: 1.001–1.025, $P = 0.032$), and miR-4497 (OR: 0.005, 95% CI:

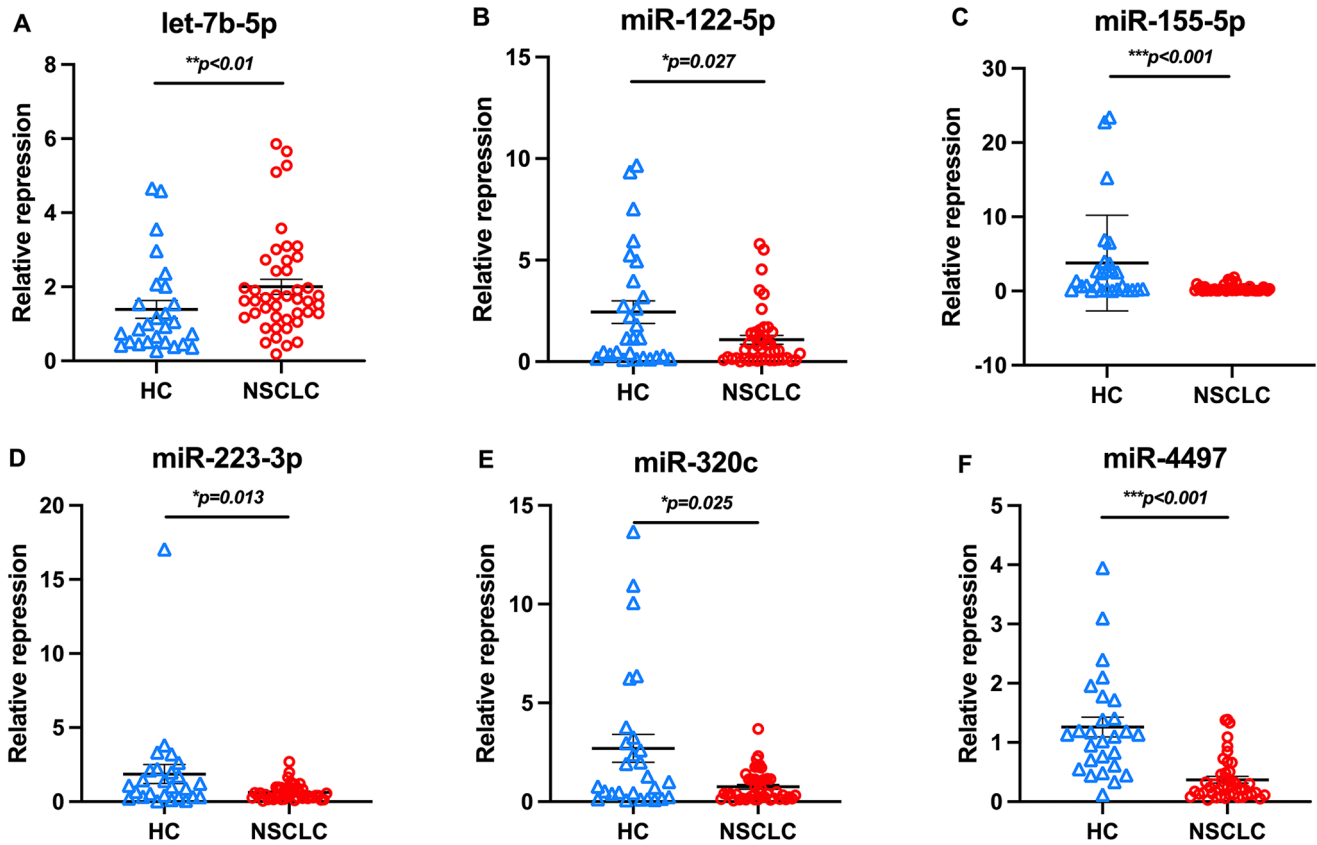


Figure 2. Relative expression levels of the serum exosomal miRNAs were assessed by qRT-PCR. The expression levels of (A) let-7b-5p, (B) miR-122-5p, (C) miR-155-5p, (D) miR-223-3p, (E) miR-320c, and (F) miR-4497 in the NSCLC patients and healthy controls (HC). * $P < 0.05$; ** $P < 0.01$; *** $P < 0.001$.

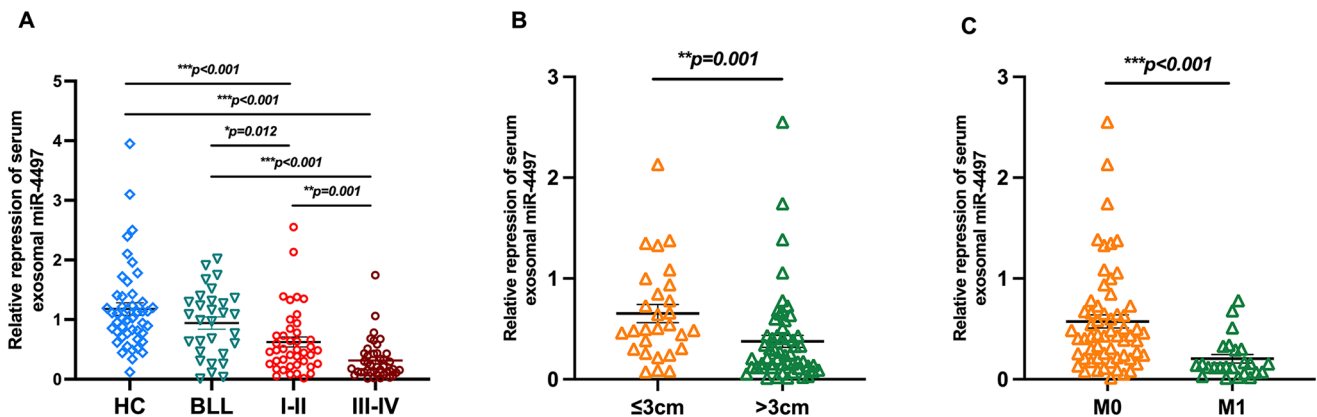


Figure 3. Serum exosomal miR-4497 is significantly downregulated in patients with NSCLC. (A) The relative repression of serum exosomal miR-4497 in healthy controls (HCs), benign lung lesion (BLL) patients, stage I–II and III–IV NSCLC patients. (B, C) The expression of exosomal miR-4497 was associated with tumor size and distant metastasis. * $P < 0.05$; ** $P < 0.01$; *** $P < 0.001$.

0.000–0.163, $P = 0.003$) were entered in the equation at the last step. These data indicate that exosomal miR-4497 acts as an independent tumor suppressor that inhibits the growth and metastasis of NSCLC.

Diagnostic and monitoring value of serum exosomal miR-4497 for NSCLC

For single biomarkers, ROC curve analysis was performed to evaluate the diagnostic accuracy of miR-4497. The AUC of

exosomal miR-4497 was 0.855, with a sensitivity of 76.6% and specificity of 83.3% for distinguishing between NSCLC and HCs (Figure 4(A)). In addition, the AUC was 0.748, with a sensitivity of 73.3% and specificity of 72.6% in discriminating NSCLC patients from BLL patients (Figure 4(B)). Comparing stage I–II NSCLC patients and HCs, the ROC curve had 76.6% sensitivity and 73.8% specificity, with an AUC of 0.784 (Figure 4(C)). According to the binary logistic results shown in Table 2, the factors that entered the binary logistic

Table 2. Regression analysis of clinical model with tumor size, TNM stage, lymph node metastasis, distant metastasis.

Clinical model	OR	<i>P</i> value	95% CI
Model 1: ≤3cm vs >3cm			
Smoking	4.688	<i>0.016</i>	1.337–16.438
miR-4497	0.243	<i>0.019</i>	0.074–0.793
Model 2: I–II vs III–IV			
NSE	1.263	<i>0.003</i>	1.085–1.469
CA125	1.077	<i>0.005</i>	1.023–1.134
miR-4497	0.155	<i>0.016</i>	0.034–0.709
Model 3: LNM(–) vs LNM(+)			
NSE	1.144	<i>0.011</i>	1.021–1.269
CA125	1.055	<i>0.007</i>	1.015–1.097
Model 4: M0 vs M1			
NSE	1.163	<i>0.010</i>	1.036–1.306
CA125	1.013	<i>0.032</i>	1.001–1.025
miR-4497	0.005	<i>0.003</i>	0.000–0.163

TNM: tumor–node–metastasis; OR: odd ratio; CI: confidence interval; miR: microRNA; NSE: neuron-specific enolase; LNM: lymph node metastasis; M0: non-distant metastasis, M1: distant metastasis. All data with *P* value of <0.05 are bolded and italicized. *P* < 0.05 was considered statistically significant.

regression equations (miR-4497 and smoking for Model 1; miR-4497, NSE, and CA125 for TNM stage for Model 2; and miR-4497, age, and CA125 for distant metastasis for Model 4) were selected as the best combinations in the following ROC analysis. In Figure 4(D), the combination of smoking and miR-4497 yielded a sensitivity of 67.9% and specificity of 78.6% for identifying tumor size (≤3 cm vs >3 cm), with an higher AUC of 0.761, compared with that of a single miR-4497. Similarly, in other models, higher diagnostic efficacies were observed owing to the combination of miR-4497 with other biomarkers. Specifically, the combination of serum exosomal miR-4497, NSE, and CA125 produced a higher AUC value of 0.878, specificity of 73.8%, and sensitivity of 85.7% compared with that of other single biomarkers for discriminating advanced stages from stages I–II (Figure 4(E)). Compared with NSCLC patients with distant metastasis (M1) and non-distant metastasis (M0), the combined ROC curve of serum exosomal miR-4497, NSE, and CA125 exhibited relatively high sensitivity (83.3%) and specificity (88.3%), with an AUC of 0.895 (Figure 4(F)). The specific data are presented in Table 3.

Subsequently, a longitudinal analysis of the progressive changes in serum exosomal miR-4497 levels was conducted in 70 patients (from 84 NSCLC patients) who received treatment, including 40 after surgery, 26 after chemoradiotherapy, and 4 after targeted therapy. In comparing serum exosome miR-4497 levels between paired samples, we observed significantly higher serum exosomal miR-4497 levels in NSCLC patients after treatment (pre vs post: 0.464 ± 0.058 vs 1.123 ± 0.250 , *P* < 0.001) (Figure 5(A)). We then grouped them according to treatment. The exosomal miR-4497 expression was significantly decreased after chemoradiotherapy compared with that pretreatment (pre vs post: 0.331 ± 0.073 vs 1.281 ± 0.459 , *P* < 0.001) (Figure 5(B)). Moreover, no significant difference was observed between patients before and after surgery (pre vs post: 0.556 ± 0.087 vs 0.667 ± 0.136 , *P* = 0.615) (Figure 5(C)).

Prognostic value of serum exosomal miR-4497 in NSCLC patients

To study the prognostic value of serum exosomal miR-4497, patients with NSCLC were followed up, and data on overall survival (OS) and disease-free survival (DFS) were obtained. OS was defined as the time from disease onset to the date of death, and DFS was calculated from the date of diagnosis until the first evidence of relapse or the last follow-up. Based on the median levels of miR-4497, we divided the 44 NSCLC patients into high- (*n* = 22) and low-expression groups (*n* = 22). Kaplan–Meier survival analysis demonstrated shorter OS (low vs high: 28.565 ± 3.815 vs 41.886 ± 2.759 months, *P* = 0.011) (Figure 6(A)) and DFS (low vs high: 24.112 ± 3.538 vs 41.283 ± 2.558 months, *P* < 0.001) (Figure 6(B)) in patients with low- versus high-serum exosomal miR-4497 levels. Therefore, miR-4497 is a protective factor in the prognosis of NSCLC patients.

Cox proportional hazards regression was used to explore the prognostic factors affecting the OS and DFS of patients with NSCLC. Univariate results revealed that OS and DFS were associated with tumor size, TNM stage, LNM, and distant metastasis and CEA, CA125, and exosomal miR-4497 levels (Table 4). After removing the influencing factors of collinearity through multiple collinearity analyses, LNM (hazard ratio [HR]: 9.317; 95% CI: 1.110–78.191; *P* = 0.040) and distant metastasis (HR: 5.970; 95% CI: 1.535–23.221; *P* = 0.010) were identified as independent risk factors for OS in NSCLC patients in the multivariate analysis. In addition, we found that CA125 (HR: 5.776, 95% CI: 1.826–18.270, *P* = 0.003) and serum exosomal miR-4497 (HR: 0.190, 95% CI: 0.055–0.659, *P* = 0.009) were independent prognostic factors for DFS in NSCLC patients (Table 4).

Discussion

LC has long been a disease with late-stage diagnosis and slow progress in treatment options,²¹ the diagnosis of which still depends on traditional imaging examinations, biopsies, or regular tumor biomarkers. Due to the inherent clinical heterogeneity, patients with LC lack typical symptoms and are easily confused with benign lesions, which leads to misdiagnosis and missed diagnosis and is not conducive to early treatment; therefore, finding suitable biomarkers remains a critical challenge in patients with LC.²² Notably, for patients with tumors discovered through screening, the need for prognostic molecular and clinical markers has not been clearly met. Exosomal miRNAs are potential non-invasive biomarkers for occurrence, development, and metastasis.²³ Based on our previous findings and a literature report, we screened six serum exosomal miRNAs that could distinguish the NSCLC group from the HC group. We then expanded the sample size and selected miR-4497 for further analysis. The results showed that serum exosomal miR-4497 had a unique diagnostic value: (1) it was most significantly decreased in NSCLC patients compared with that in BLL patients and HCs; (2) it was negatively associated with the malignant characteristics of tumors (tumor size, TNM stage, and distant metastasis) and is an independent tumor suppressor; (3) it had excellent diagnostic efficacy, which could be improved by combining it with traditional markers; and (4) it was

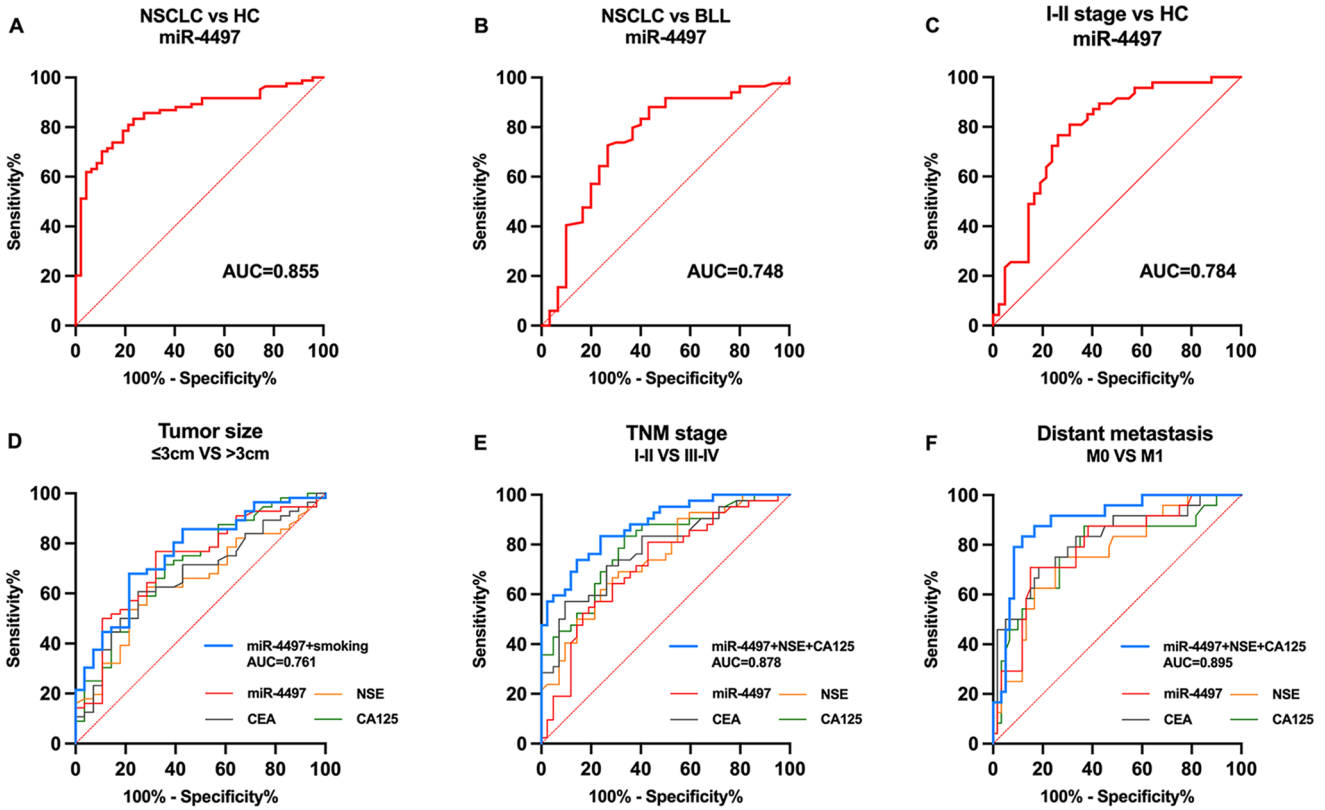


Figure 4. Diagnostic value of serum exosomal miR-4497 and clinical tumor markers for NSCLC. (A to C) ROC analysis was used to differentiate the diagnostic efficacy of serum exosomal miR-4497 expression in the NSCLC group from healthy controls and the BLL group. (D) ROC curve of single miR-4497, traditional tumor biomarkers, and combined ROC curve of Model 1. (E) ROC curve of single miR-4497, traditional tumor biomarkers, and combined ROC curve of Model 2. (F) ROC curve of single miR-4497, traditional tumor biomarkers, and combined ROC curve of Model 4.

Table 3. Diagnostic performance of serum exosomal miR-4497 and clinical biomarkers.

Clinical model	Biomarkers	<i>P</i> value	AUC	95% CI	Sensitivity (%)	Specificity (%)
Model 1: ≤3 cm vs >3 cm	miR-4497	0.001	0.725	0.610–0.840	67.9	76.8
	CEA	0.012	0.669	0.550–0.788	60.7	75.0
	NSE	0.029	0.647	0.527–0.767	62.5	71.4
	CA125	0.002	0.712	0.596–0.829	71.4	64.3
	miR-4497 + smoking	<0.001	0.761	0.655–0.868	67.9	78.6
Model 2: I-II vs III-IV	miR-4497	0.001	0.717	0.607–0.827	57.1	61.9
	CEA	<0.001	0.779	0.680–0.877	57.1	90.5
	NSE	<0.001	0.747	0.644–0.850	66.7	71.4
	CA125	<0.001	0.799	0.706–0.893	83.3	66.7
	miR-4497 + NSE + CA125	<0.001	0.878	0.808–0.948	73.8	85.7
Model 3: LNM(-) vs LNM(+)	miR-4497	0.125	0.597	0.473–0.722	57.5	65.9
	CEA	0.022	0.646	0.528–0.763	61.4	65.0
	NSE	0.001	0.709	0.598–0.819	68.2	67.5
	CA125	<0.001	0.752	0.648–0.856	61.4	82.5
	NSE + CA125	<0.001	0.817	0.728–0.906	86.4	62.5
Model 4: M0 vs M1	miR-4497	0.001	0.791	0.683–0.899	85.0	70.8
	CEA	<0.001	0.816	0.711–0.922	70.8	81.7
	NSE	<0.001	0.761	0.649–0.873	75.0	75.0
	CA125	<0.001	0.779	0.660–0.897	87.5	63.3
	miR-4497 + NSE + CA125	<0.001	0.895	0.821–0.969	83.3	88.3

AUC: area under the ROC (receiver operating characteristic) curve; CI: confidence interval; miR: microRNA; CEA: carcinoembryonic antigen; NSE: neuron-specific enolase; LNM: lymph node metastasis.

The *P* value and AUC of combined curves were bolded and italicized. *P* < 0.05 was considered statistically significant.

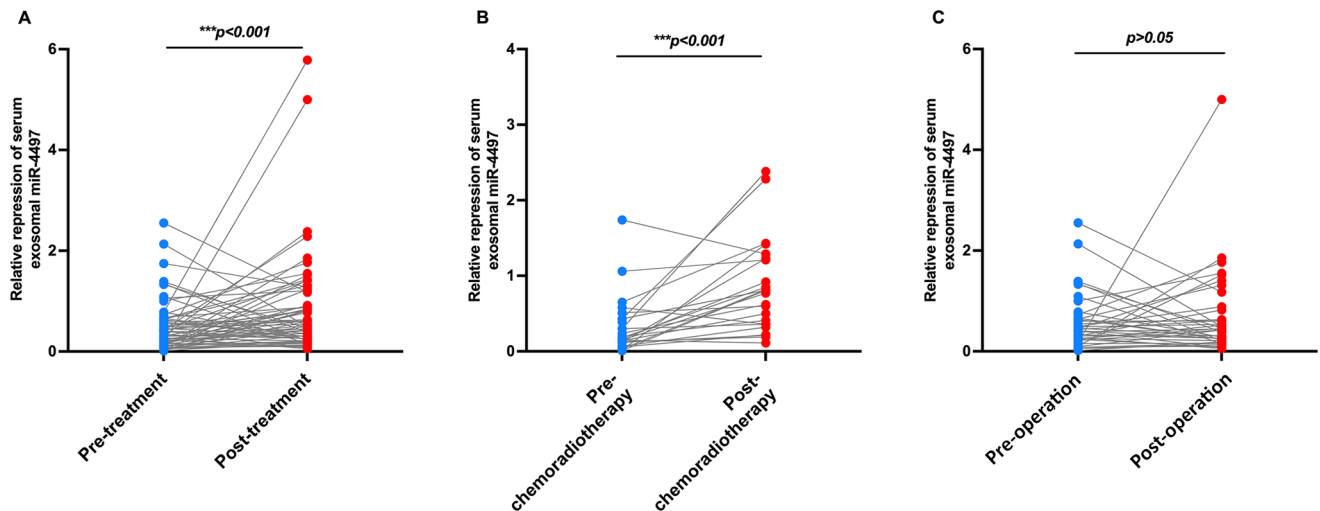


Figure 5. The progressive changes of exosomal miR-4497 following treatment. (A) Serum exosomal miR-4497 was significantly increased following treatment. (B) Serum exosomal miR-4497 was significantly increased after chemoradiotherapy. (C) Comparison of serum exosomal miR-4497 expression before and after operation in NSCLC patients.

* $P < 0.05$; ** $P < 0.01$; *** $P < 0.001$.

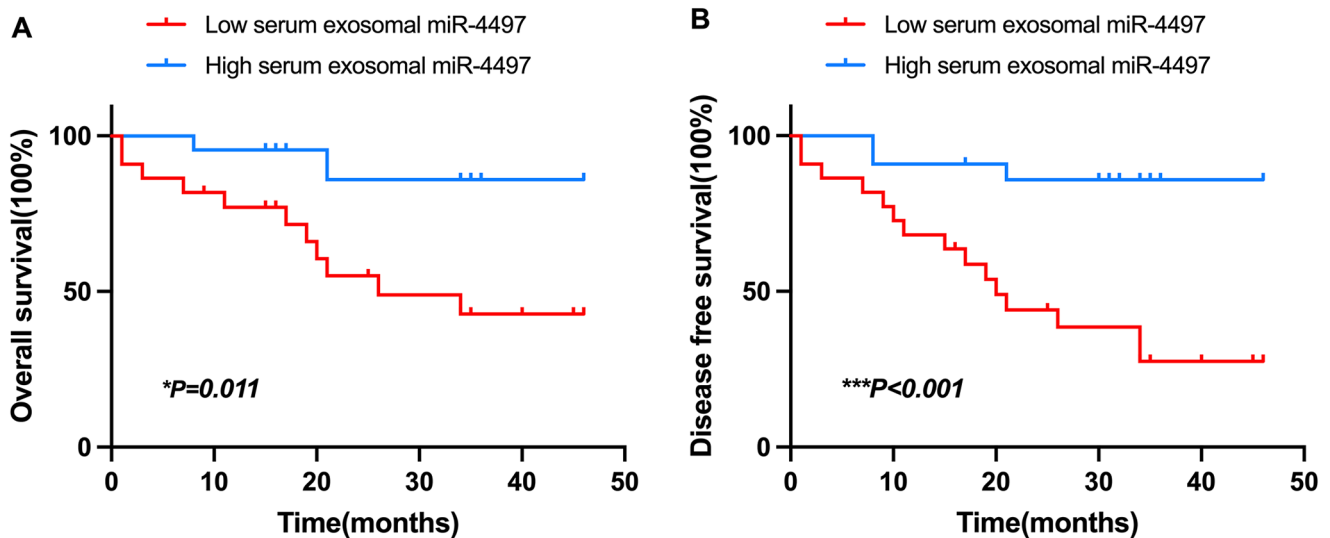


Figure 6. Serum exosomal miR-4497 were prognostic factors in patients with NSCLC. (A) Low-serum exosomal miR-4497 expression was correlated with shorter OS. (B) Low-serum exosomal miR-4497 expression was correlated with shorter DFS.

* $P < 0.05$; ** $P < 0.01$; *** $P < 0.001$.

useful for therapeutic monitoring and may be a protective factor for OS and DFS in NSCLC.

Our results indicate that exosomal miR-4497 could be an independent tumor suppressor that inhibits the growth and metastasis of NSCLC. In addition, some previous studies at the cellular and molecular levels have provided direct or indirect evidence that miR-4497 may be related to the inhibition of the proliferation and progression of LC. MiR-4497 has an indirect and obvious killing effect on LC cells by regulating target genes and their related pathways. For instance, the level of miR-4497 in NSCLC tissues is significantly lower than that in normal lung tissues. In addition, silencing MED13L by upregulating miR-4497 can reduce PRKCA gene expression, thereby enhancing the cytotoxic effect of radiation therapy *in vitro* and *in vivo*.²⁰ Similarly, in a lung squamous

cell carcinoma (LSCC) cell model, FEZF1-AS1 enhanced the viability, migration, and invasion of LSCC cells by down-regulating the inhibitory effects of miR-4497 on GBX2.^{24,25} In contrast, miR-4497 inhibited progression and metastasis via an indirect immune-inflammatory microenvironment. This assumption is based on previous findings that miR-4497 can induce human monocytes to express and secrete tumor necrosis factor α ,²⁶ and can be upregulated by ultraviolet B to increase the inflammatory and oxidative stress signals.²⁷ However, most studies on miR-4497 in tumors have focused on its mechanism of action, and few studies have reported that exosomal miR-4497 could be a circulating biomarker. To date, only one study has been published on exosomal miR-4497 in human breast milk,²⁶ with no reports on the use of exosomal miRNAs to discriminate NSCLC from BLL,

Table 4. Univariate and multivariate analysis of the impact of possible risk factors on DFS in NSCLC patients.

Parameters	Univariate analysis					
	OS			DFS		
	HR	95% CI	P value	HR	95% CI	P value
Age	1.317	0.438–3.966	0.624	1.139	0.443–2.930	0.787
Gender	2.298	0.508–10.395	0.280	3.472	0.796–15.144	0.098
Smoking	0.927	0.255–3.371	0.927	0.847	0.279–2.574	0.769
Hypertension	0.282	0.037–2.175	0.225	0.737	0.212–2.563	0.631
Diabetes mellitus	1.303	0.288–5.887	0.731	0.899	0.206–3.916	0.887
Primary location	1.209	0.395–3.703	0.739	0.702	0.278–1.771	0.454
Tumor size	7.276	0.944–56.079	0.057	5.102	1.169–22.275	0.030
Pathological classification	1.906	0.422–8.614	0.402	1.132	0.371–3.460	0.828
TNM stage	2.479	1.262–4.939	0.009	7.130	2.037–24.957	0.002
Lymph node metastasis	17.875	2.296139.182	0.006	5.027	1.633–15.478	0.005
Distant metastasis	11.592	3.113–43.160	< 0.001	4.050	1.570–10.445	0.004
Mutation	1.581	0.516–4.851	0.423	1.179	0.442–3.148	0.742
CEA	4.026	1.106–14.652	0.035	1.805	0.699–4.660	0.222
NSE	2.407	0.740–7.827	0.144	1.316	0.518–3.343	0.563
CA125	5.973	1.591–22.421	0.008	6.002	1.923–18.729	0.002
miR-4497	0.178	0.039–0.804	0.025	0.179	0.052–0.619	0.007

Parameters	Multivariate analysis					
	OS			DFS		
	HR	95% CI	P value	HR	95% CI	P value
Lymph node metastasis	9.317	1.110–78.191	0.040	–	–	–
Distant metastasis	5.970	1.535–23.221	0.010	–	–	–
CA125	–	–	–	5.776	1.826–18.270	0.003
miR-4497	–	–	–	0.190	0.055–0.659	0.009

NSCLC: non-small-cell lung cancer; OS: overall survival; DFS: disease-free survival; HR: hazard ratio; CI: confidence interval; TNM: tumor–node–metastasis; CEA: carcinoembryonic antigen; NSE: neuron-specific enolase; miR: microRNA.

All data with *P* value of <0.05 are bolded and italicized. *P* < 0.05 was considered statistically significant.

which is closely associated with LC occurrence and development.²⁸ In addition, most traditional biomarkers are tumor promoters and rarely provide specific and early diagnostic value for LC.²⁹ Thus, we studied the expression characteristics of miR-4497 in circulating exosomes in NSCLC for the first time, which showed excellent antitumor effects in the identification of multiple models, whether in early screening to identify NSCLC, BLL, and healthy people, or in staging, grading, prognosis, and monitoring of recurrence, metastasis, and the therapeutic effects in patients with NSCLC. Notably, our study showed that miR-4497 packaged in circulating exosome was an independent tumor suppressor, and when combined with tumor markers can provide high diagnostic accuracy in discriminating the TNM stage and its determining parameters (tumor size and distant metastasis). Therefore, our results suggest that serum exosomal miR-4497 has excellent clinical application value and could be a good circulating biomarker for establishing optimal combination panels to screen and diagnose NSCLC.

Tumor mutational burden (TMB) has emerged as an independent biomarker for predicting patient response to immune checkpoint inhibitor treatment.^{30,31} The expression patterns of miRNAs are related to TMB, and miRNA-based signature classifiers could serve as biomarkers to predict

TMB levels in patients with NSCLC.³² Moreover, the low survival rates and poor prognosis of LC patients have always been problematic.^{33,34} Hence, identifying the ideal miRNA biomarkers is necessary for effective monitoring and to improve the therapeutic outcome of patients with NSCLC, especially patients with advanced LC. In our study, serum exosomal miR-4497 levels significantly increased after chemoradiotherapy, indicating that it can be used as a marker for the reduction of tumor burden in certain therapeutic schedules. Moreover, for the first time, we found that as an independent prognostic protective factor, miR-4497 was closely correlated with OS and DFS in patients with NSCLC. Thus, effectively monitoring the prognosis of patients is possible. These findings are consistent with those of previous studies showing that elevated serum miR-4497 expression is associated with increased progression-free survival and OS in patients with locally advanced NSCLC after radiotherapy.²⁰

In conclusion, our findings revealed for the first time that serum exosomal miR-4497 was downregulated in NSCLC patients compared with BLL patients and HCs, and its expression was negatively related to the malignant characteristics of tumors (tumor size, TNM stage, and distant metastasis), acting as an independent tumor suppressor with excellent clinical diagnostic and treatment monitoring

value. In addition, a decrease in serum exosomal miR-4497 was associated with diminished survival and poor prognosis in patients with NSCLC. Thus, our data demonstrate that serum exosomal miR-4497 is a promising biomarker for early screening, staging, and grading, as well as monitoring recurrence, metastasis, prognosis, and therapeutic effects in patients with NSCLC. However, further studies are needed to validate exosomal miR-4497 with much larger sample sizes and other testing facilities. Furthermore, the mechanism of serum exosomal miR-4497 in patients with NSCLC warrants further investigation.

AUTHORS' CONTRIBUTIONS

All authors participated in the study protocol design, experimental process, data analysis, and manuscript review. YTT and YRL designed the research; BKZ and MCP performed the experiments and wrote the paper; JG, CSL, and HBC collected clinical data and samples; BKZ performed the statistical analysis; and BKZ and YTT revised the paper.

ACKNOWLEDGEMENTS

The authors thank Dr Jiayu Sun for her support with biostatistical analysis.

DECLARATION OF CONFLICTING INTERESTS

The author(s) declared no potential conflicts of interest with respect to the research, authorship, and/or publication of this article.

FUNDING

The author(s) disclosed receipt of the following financial support for the research, authorship, and/or publication of this article: This study was funded by the Natural Science Foundation of Hubei Province (Grant No. 2021CFB415) and the Youth Interdisciplinary Special Fund of the Zhongnan Hospital of Wuhan University (Grant No. ZNQNJC2022008), National Natural Science Foundation of China (Grant No. 81702273), and Zhongnan Hospital of Wuhan University Science, Technology and Innovation Seed Fund, Projects znp2018117 and znp2019064.

ORCID ID

Bokun Zheng  <https://orcid.org/0000-0001-7333-7016>

REFERENCES

- Siegel RL, Miller KD, Fuchs HE, Jemal A. Cancer statistics, 2022. *CA Cancer J Clin* 2022;**72**:7–33
- Thai AA, Solomon BJ, Sequist LV, Gainor JF, Heist RS. Lung cancer. *Lancet* 2021;**398**:535–54
- Brody H. Lung cancer. *Nature* 2020;**587**:S7
- Nooreldeen R, Bach H. Current and future development in lung cancer diagnosis. *Int J Mol Sci* 2021;**22**:8661
- Mathios D, Johansen JS, Cristiano S, Medina JE, Phallen J, Larsen KR, Bruhm DC, Niknafs N, Ferreira L, Adleff V, Chiao JY, Leal A, Noe M, White JR, Arun AS, Hruban C, Annapragada AV, Jensen S, Ørntoft MW, Madsen AH, Carvalho B, de Wit M, Carey J, Dracopoli NC, Maddala T, Fang KC, Hartman AR, Forde PM, Anagnostou V, Brahmer JR, Fijneman RJA, Nielsen HJ, Meijer GA, Andersen CL, Mellemegaard A, Bojesen SE, Scharpf RB, Velculescu VE. Detection and characterization of lung cancer using cell-free DNA fragmentomes. *Nat Commun* 2021;**12**:5060
- Chemi F, Rothwell DG, McGranahan N, Gulati S, Abbosh C, Pearce SP, Zhou C, Wilson GA, Jamal-Hanjani M, Birkbak N, Pierce J, Kim CS, Ferdous S, Burt DJ, Slane-Tan D, Gomes F, Moore D, Shah R, Al Bakir M, Hiley C, Veeriah S, Summers Y, Crosbie P, Ward S, Mesquita B, Dynowski M, Biswas D, Tugwood J, Blackhall F, Miller C, Hackshaw A, Brady G, Swanton C, Dive C. Pulmonary venous circulating tumor cell dissemination before tumor resection and disease relapse. *Nat Med* 2019;**25**:1534–9
- Liu J, Ren L, Li S, Li W, Zheng X, Yang Y, Fu W, Yi J, Wang J, Du G. The biology, function, and applications of exosomes in cancer. *Acta Pharm Sin B* 2021;**11**:2783–97
- Théry C, Zitvogel L, Amigorena S. Exosomes: composition, biogenesis and function. *Nat Rev Immunol* 2002;**2**:569–79
- Milane L, Singh A, Mattheolabakis G, Suresh M, Amiji MM. Exosome mediated communication within the tumor microenvironment. *J Control Release* 2015;**219**:278–94
- Zhang L, Yu D. Exosomes in cancer development, metastasis, and immunity. *Biochim Biophys Acta Rev Cancer* 2019;**1871**:455–68
- Kalluri R, LeBleu VS. The biology, function, and biomedical applications of exosomes. *Science* 2020;**367**:eaa06977
- Xia B, Gao J, Li S, Huang L, Zhu L, Ma T, Zhao L, Yang Y, Luo K, Shi X, Mei L, Zhang H, Zheng Y, Lu L, Luo Z, Huang J. Mechanical stimulation of Schwann cells promote peripheral nerve regeneration via extracellular vesicle-mediated transfer of microRNA 23b-3p. *Theranostics* 2020;**10**:8974–95
- Bartel DP. MicroRNAs: target recognition and regulatory functions. *Cell* 2009;**136**:215–33
- Sun Z, Shi K, Yang S, Liu J, Zhou Q, Wang G, Song J, Li Z, Zhang Z, Yuan W. Effect of exosomal miRNA on cancer biology and clinical applications. *Mol Cancer* 2018;**17**:147
- Tang YT, Huang YY, Li JH, Qin SH, Xu Y, An TX, Liu CC, Wang Q, Zheng L. Alterations in exosomal miRNA profile upon epithelial-mesenchymal transition in human lung cancer cell lines. *BMC Genomics* 2018;**19**:802
- Jin X, Chen Y, Chen H, Fei S, Chen D, Cai X, Liu L, Lin B, Su H, Zhao L, Su M, Pan H, Shen L, Xie D, Xie C. Evaluation of tumor-derived exosomal miRNA as potential diagnostic biomarkers for early-stage non-small cell lung cancer using next-generation sequencing. *Clin Cancer Res* 2017;**23**:5311–9
- Xue MY, Cao HX. LINC01551 promotes metastasis of nasopharyngeal carcinoma through targeting microRNA-132-5p. *Eur Rev Med Pharmacol Sci* 2020;**24**:3724–33
- Luo P, Wang Q, Ye Y, Zhang J, Lu D, Cheng L, Zhou H, Xie M, Wang B. MiR-223-3p functions as a tumor suppressor in lung squamous cell carcinoma by miR-223-3p-mutant p53 regulatory feedback loop. *J Exp Clin Cancer Res* 2019;**38**:74
- Zhu L, Xue F, Cui Y, Liu S, Li G, Li J, Guan B, Zeng H, Bian W, Yang C, Zhao C. miR-155-5p and miR-760 mediate radiation therapy suppressed malignancy of non-small cell lung cancer cells. *Biofactors* 2019;**45**:393–400
- Zhang N, Song Y, Xu Y, Liu J, Shen Y, Zhou L, Yu J, Yang M. MED13L integrates Mediator-regulated epigenetic control into lung cancer radiosensitivity. *Theranostics* 2020;**10**:9378–94
- Hirsch FR, Scagliotti GV, Mulshine JL, Kwon R, Curran WJ Jr, Wu YL, Paz-Ares L. Lung cancer: current therapies and new targeted treatments. *Lancet* 2017;**389**:299–311
- Seijo LM, Peled N, Ajona D, Boeri M, Field JK, Sozzi G, Pio R, Zulueta JJ, Spira A, Massion PP, Mazzone PJ, Montuenga LM. Biomarkers in lung cancer screening: achievements, promises, and challenges. *J Thorac Oncol* 2019;**14**:343–57
- Hu C, Meiners S, Lukas C, Stathopoulos GT, Chen J. Role of exosomal microRNAs in lung cancer biology and clinical applications. *Cell Prolif* 2020;**53**:e12828
- Chen X, Zhang L, Tang S. MicroRNA-4497 functions as a tumor suppressor in laryngeal squamous cell carcinoma via negatively modulation of the GBX2. *Auris Nasus Larynx* 2019;**46**:106–13
- Chen X, Cheng P, Hu C. LncRNA FEZF1-AS1 accelerates the migration and invasion of laryngeal squamous cell carcinoma cells through miR-4497 targeting GBX2. *Eur Arch Otorhinolaryngol* 2021;**278**:1523–35

26. Mirza AH, Kaur S, Nielsen LB, Størling J, Yarani R, Roursgaard M, Mathiesen ER, Damm P, Svare J, Mortensen HB, Pociot F. Breast milk-derived extracellular vesicles enriched in exosomes from mothers with type 1 diabetes contain aberrant levels of microRNAs. *Front Immunol* 2019;**10**:2543
27. Yang L, Hu Z, Jin Y, Huang N, Xu S. MiR-4497 mediates oxidative stress and inflammatory injury in keratinocytes induced by ultraviolet B radiation through regulating NF- κ B expression. *Ital J Dermatol Venereol* 2022;**157**:84–91
28. Hou W, Hu S, Li C, Ma H, Wang Q, Meng G, Guo T, Zhang J. Cigarette smoke induced lung barrier dysfunction, EMT, and tissue remodeling: a possible link between COPD and lung cancer. *Biomed Res Int* 2019;**2019**:2025636
29. Duffy MJ, O'Byrne K. Tissue and blood biomarkers in lung cancer: a review (Chapter 1). In: Makowski GS (ed.) *Advances in clinical chemistry*. Amsterdam: Elsevier, 2018, pp. 1–21
30. Hellmann MD, Ciuleanu TE, Pluzanski A, Lee JS, Otterson GA, Audigier-Valette C, Minenza E, Linardou H, Burgers S, Salman P, Borghaei H, Ramalingam SS, Brahmer J, Reck M, O'Byrne KJ, Geese WJ, Green G, Chang H, Szustakowski J, Bhagavatheeswaran P, Healey D, Fu Y, Nathan F, Paz-Ares L. Nivolumab plus ipilimumab in lung cancer with a high tumor mutational burden. *N Engl J Med* 2018;**378**:2093–104
31. Carbone DP, Reck M, Paz-Ares L, Creelan B, Horn L, Steins M, Felip E, van den Heuvel MM, Ciuleanu TE, Badin F, Ready N, Hiltermann TJJ, Nair S, Juergens R, Peters S, Minenza E, Wrangle JM, Rodriguez-Abreu D, Borghaei H, Blumenschein GR Jr, Villaruz LC, Havel L, Krejci J, Corral Jaime J, Chang H, Geese WJ, Bhagavatheeswaran P, Chen AC, Socinski MA First-line nivolumab in stage IV or recurrent non-small-cell lung cancer. *N Engl J Med* 2017;**376**:2415–26
32. Lv Y, Huang Z, Lin Y, Fang Y, Chen Z, Pan L, Zhang Y, Xu Z. MiRNA expression patterns are associated with tumor mutational burden in lung adenocarcinoma. *Oncoimmunology* 2019;**8**:e1629260
33. Chen Z, Fillmore CM, Hammerman PS, Kim CF, Wong KK. Non-small-cell lung cancers: a heterogeneous set of diseases. *Nat Rev Cancer* 2014;**14**:535–46
34. Jones GS, Baldwin DR. Recent advances in the management of lung cancer. *Clin Med* 2018;**18**:s41–6

(Received October 9, 2022, Accepted April 12, 2023)